Research Square

Preprints are preliminary reports that have not undergone peer review.
They should not be considered conclusive, used to inform clinical practice,
or referenced by the media as validated information.

Light-dependent aggregate formation and photosynthetic acclimation during biofilm development in Synechocystis sp. PCC 6803

Mariann Kis

kis.mariann@blki.hun-ren.hu

HUN-REN Balaton Limnological Research Institute

Attila W. Kovács

HUN-REN Balaton Limnological Research Institute

Gábor Bernát

HUN-REN Balaton Limnological Research Institute

Research Article

Keywords: cyanobacterial biofilm, cell aggregate formation, DIC microscopy, EPS determination, log-normal distribution, PSII photochemistry

Posted Date: June 24th, 2026

DOI: https://doi.org/10.21203/rs.3.rs-9994848/v1

License: This work is licensed under a Creative Commons Attribution 4.0 International License.
Read Full License

Additional Declarations: No competing interests reported.

Version of Record: A version of this preprint was published at Microbial Ecology on September 30th, 2026. See the published version at https://doi.org/10.1007/s00248-026-02889-x.

Abstract

Biofilm formation is an important adaptive strategy for cyanobacteria in ever-changing environments. In response to shifts in the light regime, the model cyanobacterium *Synechocystis* sp. PCC 6803 GT-L can switch from a planktonic lifestyle to form a phototrophic biofilm. Planktonic cultures contain single cells and microcolonies, whereas developing biofilms are dominated by cell aggregates with remarkable heterogeneity. Distribution analysis revealed that aggregate areas increased under higher irradiance (250–400 μmol photons m^{-2} s^{-1}) and exhibited a strong wavelength dependence, reaching maximum values under blue-greenish light (460–510 nm) and minimum values under yellow-orange wavelengths (560–590 nm). Extracellular polymeric substance (EPS) production closely followed the aggregation pattern. Biofilm cultures produced significantly higher levels of EPS than planktonic cultures, with cultivation under blue light inducing the highest EPS accumulation. Switching the cultivation light between red (630 nm) and blue (460 nm) demonstrated that EPS production and aggregate formation are reversible and actively regulated by the light regime. Growth rates and EPS production showed the opposite patterns: cultures grown under 630 nm light exhibited the highest growth rates and minimal EPS secretion, whereas cultures grown under 460 nm light showed the lowest growth rate and maximal EPS secretion. Chlorophyll fluorescence parameters derived from OJIP curves revealed that biofilm-associated cells had a smaller pool size of electron acceptors (S_M), a reduced maximum photochemical efficiency (φP_0), an increased apparent antenna size of PSII (ABS/RC), and enhanced energy dissipation (DI_0/RC) relative to planktonic cells. In contrast, biofilm-associated cells maintained relatively high φP_0 and reduced ABS/RC and DI_0/RC grown under violet-green (430–540 nm) wavelengths, whereas planktonic cells showed excitation-induced stress. These results demonstrate the central role of light-regulated physiological plasticity in cyanobacterial biofilm development.

Introduction

One of the most studied microorganisms, the cyanobacterium *Synechocystis sp*. PCC 6803 (hereafter referred to as *Synechocystis*; Kaneko et al., 1996; Ikeuchi and Tabata, 2001) is commonly used in laboratory experiments to study photosynthetic electron transport, stress acclimation, redox regulation, and carbon and nitrogen metabolism (Allen, 2014; Burnap et al., 2015). In addition, *Synechocystis* has also been used as a model organism to study microbial connectivity and surface-associated lifestyles. Despite its unicellular nature, it readily forms aggregates, flocculated forms, and surface-adherent biofilms under various laboratory and environmental conditions (Jittawuttipoka et al., 2013; Allen et al., 2019).

Some microorganisms often switch between a free-living planktonic state and a surface-associated biofilm lifestyle; such a transition strongly alters cellular physiology, gene expression patterns, and ecological performance (Costerton et al., 1995; Flemming and Wingender, 2010). Biofilms are structured microbial communities embedded in an extracellular polymer matrix produced by the cells, which are either attached to biotic or abiotic surfaces or exist as aggregates. Phototrophic biofilms develop gradients (depending on light, oxygen, inorganic carbon, and nutrient availability), resulting in

heterogeneity in cellular metabolism, growth, and division (Stal, 1995; de Beer et al., 1997). In *Synechocystis*, the transition between planktonic growth and biofilm formation can be triggered by environmental changes such as light conditions, nutrient availability, ionic strength, and surface properties (Jittawuttipoka et al., 2013; Allen et al., 2019). Cell wall proteins and the produced extracellular polymer trigger cell-to-cell cohesion and surface adhesion (Bhaya et al., 2002; Fisher et al., 2013).

A fundamental element of biofilms is the extracellular polymeric substance (EPS), which, together with the cells, creates a matrix that provides stability and a boundary between the cells and their environment (Flemming and Wingender, 2010). The EPS produced by cyanobacteria is predominantly composed of polysaccharides and often contains proteins, nucleic acids, and lipids (De Philippis et al., 2001; Pereira et al., 2015). Through its structural features, EPS also protects cells from desiccation and freezing, participates in the diffusion and storage of gases and nutrients, and provides protection against high light intensity and oxidative stress (De Philippis and Vincenzini, 1998; Tamaru et al., 2005).

Microbial biofilms are structurally heterogeneous under both natural and laboratory-controlled conditions. They contain single cells, dividing cells, microcolonies, and clusters of cells of various sizes and shapes. Due to this high degree of variability, the size distribution of these aggregates usually does not follow normal distribution. Rather, the cluster size distribution of biofilms can often be described by log-normal functions, among other distribution functions (Hirano et al., 1982; Tsagkari et al., 2022). Although several multiplicative processes (growth, adhesion, detachment, and the merging of aggregates) occur during biofilm formation, the log-normal distribution is well suited to describe both natural and laboratory-grown biofilm structures. Parameters derived from the corresponding fits (e.g., mean (μ) and variance (σ)) characterize both the cluster size distribution and the extent of structural heterogeneity, thereby enabling comparisons between different laboratory treatments or environmental conditions.

Light, besides being the primary energy source of phototrophic organisms (and thus the entire food web), is also the most important environmental factor regulating photosynthesis and growth. In the case of biofilms, light also plays a major role in community organization. Light intensity directly controls the rate of photosynthesis, adjusts the redox balance and nutrient distribution, and regulates the formation of the biofilm matrix, while high light intensities may cause photoinhibition and oxidative stress (Murata et al., 2007; Hihara et al., 2001). In biofilms, outer cells provide shading for the inner ones, and the EPS matrix itself scatters light. Together, these processes create vertical light gradients and microscopic domains with different physiological states (Stal, 1995; Kühl et al., 1997). In addition to light intensity, light quality also varies within biofilms. In natural environments, where microbial mats and benthic biofilms are common, spectral filtering results in wavelength-dependent niches, potentially promoting aggregation and biofilm formation as strategies to optimize light harvesting and photoprotection (Sand-Jensen, 2014; Helbling et al., 2015).

Phenotypes of *Synechocystis* sp. PCC 6803 differs substantially among laboratory strains and has become an important aspect of studies investigating motility, EPS production, and biofilm formation. The glucose-tolerant (GT) strain commonly used in photosynthesis research. GT strain has lost the ability to synthesize synecan (Maeda K. et al. 2021), as well as its motility, while retaining the ability (also examined in this study) to adhere to abiotic surfaces and form biofilms, especially on glass surfaces. Despite the absence of synechan, GT strains still produce substantial amounts of EPS, including soluble extracellular polysaccharides released into the medium, and cell-associated polysaccharides surrounding the cell surface, with the latter being involved in adhesion and biofilm formation. Adhesion is not constitutive, but is primarily induced by environmental stress factors. GT strains are typically non-motile, although they possess thin pili (Bhaya et al., 2000; Koskinen et al., 2023) and can exhibit light-dependent phototaxis responses, but lack the thicker pili and motility apparatus found in wild-type Pasteur Collection (PCC) strains (Bhaya et al., 2000; Chen et al., 2020).

This work combines multi-intensity and multi-wavelength light treatments with biofilm-specific measurements to investigate the biofilm formation of *Synechocystis*, revealing physiological and photobiological features not observed in planktonic cultures.

In this work, we study the planktonic *vs.* biofilm lifestyle, reversible biofilm shaping, aggregate formation, EPS production, and photosystem II (PSII) photochemistry of the unicellular cyanobacterium *Synechocystis* sp. PCC 6803 GT-L over a photon flux density (PFD) range of 10–400 µmol photons m^{-2} s^{-1} and across the entire photosynthetically active radiation (PAR) spectrum, from 430 nm to 690 nm. We systematically analyzed differential interference contrast micrographs from planktonic and biofilm cultures grown under different light regimes. These micrographs were subsequently used for quantitative morphometric analysis (log-normal distribution of aggregates) and EPS determination (*via* colorimetric assay) under different treatments. Furthermore, we systematically compared OJIP fluorescence parameters between planktonic and biofilm *Synechocystis* cultures.

Materials and Methods

Strain and cultivation: *Synechocystis* sp. PCC 6803 GT-L (Zavřel et al. 2015, 2017) cells were grown in Erlenmeyer flasks at a constant temperature of 26°C in liquid BG-11 medium (Stanier et al. 1971) in an algal culture room. The stock and pre-cultivated cultures were grown under warm-white fluorescent lamps providing a photon flux density (PFD) of 25 µmol photons m^{-2} s^{-1}. The flasks containing planktonic (suspended, non-biofilm) cultures and glass beads (diameter: 2–3 mm) were placed on an orbital shaker (50 rpm) to maintain suspension homogeneity, while the biofilm cultures were left undisturbed (i.e. unshaken and without beads) on the cultivation bench until sampling.

For the light quantity acclimation experiments, the cultures were illuminated with diffuse warm-white light at intensities of 10, 25, 50, 100, 250, and 400 µmol photons m^{-2} s^{-1}. For the light quality acclimation experiments, the cultures were illuminated by monochromatic light emitting diodes (LEDs) with nine different peak wavelengths (430, 460, 510, 540, 560, 590, 630, 660, and 690 nm) under the

same PFD of 25 µmol photons m^{-2} s^{-1}. Illumination was provided as diffuse light from underneath the flasks using a home-built cultivation apparatus (Bernát et al. 2021; Zavřel et al. 2024; Kis et al. 2026). The light regime was set to a 14h:10h (light:dark) cycle, and the cultures were grown to the late-exponential phase (OD_{750} = 0.7–0.8), characterized by active cell division and biofilm formation. Growth and sampling data are provided in Supplementary Table 1.

Differential Interference Contrast (DIC) microscopy

The different phases of cellular growth, aggregate development, and biofilm formation of *Synechocystis* under different light regimes were tracked by light microscopy. Prior to imaging, the cultures were fixed with 4% glutaraldehyde for 3 h to preserve the aggregated structure. After the fixation step, the samples were detached from the glass surface by gentle pipetting. 20 µL aliquot of each sample was pipetted onto a microscope slide and covered by a coverslip (20 × 20 mm). DIC images were recorded using an Olympus BX51 microscope with a Differential Interference Contrast optical configuration, equipped with a high-performance DP75 digital microscope camera (Olympus). Twenty randomly selected fields of view were recorded for each sample. Images were captured using Olympus cellSens Dimension software (version 4.2.1) in grayscale mode to enhance structural contrast at a resolution of 2048 × 1500 pixels. Altogether, about 200–400 objects were detected in each image and used to quantify morphological parameters.

Determination of the aggregate areas: Aggregate areas on DIC images were determined using the Fiji/ImageJ open-source Java-based image processing software (version 1.46r) (Schindelin et al. 2012.). Prior to analysis, the spatial scale was set to 2.9 pixels per µm for all images, according to the microscope setup. To minimize user bias and maximize reproducibility, an ImageJ macro was written to automate object analysis (see Supplementary Text). The steps of the workflow were as follows: (1) converting images to 8-bit, (2) thresholding and masking, (3) hole-filling and watershed segmentation, and (4) particle analysis. Additionally, the macro specified a minimum (3 µm²) and maximum (3000 µm²) object size threshold to exclude cell debris and extremely large, biologically irrelevant, fused aggregates from the analysis.

Log-Normal Distribution modeling

To determine the size distribution of cellular aggregates, we evaluated the calculated area data (see above) using a log-normal distribution model. Approximately 1000 to 3000 objects (i.e. single cells, microcolonies, and aggregates) were initially detected from the images obtained from each treatment. Small objects corresponding to single cells (~ 3 µm²) and microcolonies (3–5 cells) were excluded from further analysis using a lower cutoff of ≥ 10 µm² (Rochex and Lebeault 2007). We also used percentile trimming (lower 95%) to remove large outliers (i.e., merged clusters). The remaining 200 to 600 objects per treatment were used to fit a log-normal distribution. This fitting yielded cumulative distribution function (CDF) curves, as well as the mean values (µ), standard deviation (σ), and shape parameters in log-space. The arithmetic mean in linear-space was back-transformed using standard expression exp(µ

+ $\sigma^2/2$) for the log-normal distribution. These parameters were used to compare aggregate size characteristics of cultures grown under different light regimes.

EPS isolation from fresh Synechocystis cultures

The isolation procedure accounts for both the EPS dissolved in the growth medium and the EPS bound to the cells. From each Erlenmeyer flask, a 1 mL homogeneous cell suspension was aliquoted using wide-bore pipette tips (pipetting slowly 10 times) and then centrifuged at 5000 *g* for 10 min at room temperature. To prevent cell lysis, fresh cultures were processed quickly and centrifuged gently. The remaining supernatant contained soluble EPS (chlorophyll-*a* spectra were recorded in the supernatant to check for cell lysis and avoid interference from sugar derivatives). The pellet was then gently resuspended in Tris-HCl (pH 7.5, 10 mM) and shaken (100 rpm) at room temperature for 60 min to release bound EPS (Keithley and Kirisits 2018). A subsequent centrifugation step (5000 *g*, 15 min, room temperature) was performed to separate the solubilized EPS from the cells. The collected supernatants (containing the soluble and released EPS, respectively) were used for EPS determination using a colorimetric assay (see below). The pellets containing intact, EPS-free, separated cells were resuspended in 1 mL of BG-11 medium, and their corresponding OD_{750} values were measured using a double-beam spectrophotometer (Specord 210 Plus, Analytik Jena, Jena, Germany) as a proxy for biomass.

Colorimetric assay for EPS determination: As EPS is mostly composed of polysaccharides (exopolysaccharides), colorimetric methods for carbohydrate determination are a suitable approach for EPS quantification. The EPS content of the obtained supernatants (see above) was precipitated with 100% ice-cold ethanol (1:1, v/v) and incubated overnight at 4°C. After this ethanol treatment, the samples were dried at 40–45°C, followed by the rapid addition of a reagent solution consisting of 200 µL of sterile distilled water, 200 µL of 5% phenol, and 1 mL of concentrated sulfuric acid (Dubois et al. 1956, Kis et al. 2018). After a 10 min incubation for color development in the dark and cooling in a water bath at 22°C, the optical density was determined using a double-beam Specord 210 Plus spectrophotometer at 490 nm. For quantitative assessment of the EPS content, this colorimetric method was calibrated using a series of glucose solutions of known concentrations (0, 2, 5, 10, and 20 µg/mL). To avoid any possible interference from substances other than glucose, corrections were made by running a parallel assay without the addition of phenol.

PSII photochemistry: Rapid chlorophyll fluorescence induction (OJIP) curves of light-acclimated cultures were recorded using an AquaPen fluorometer (Photon System Instruments, Brno, Czechia) by applying 620 nm saturation pulses at a PFD of 3000 µmol photons m^{-2} s^{-1}. The cultures were homogenized by gentle pipetting before measurement. From the OJIP curves, the following parameters were retrieved: F_O, F_J, F_I and F_M, referring to the fluorescence yields at the O, J, I and P points of the transient, respectively. These parameters were used to calculate the following parameters: (1) the maximum quantum yield of PSII photochemistry, φP_O (= F_V/F_M = $(F_M-F_O)/F_M$); (2) the normalized area above the OJIP curve, S_M (= Area/(F_M-F_O)), which is proportional to the pool size of electron acceptors in the photosynthetic electron

transport chain; (3) the apparent antenna size per active PSII (ABS/RC = $(M_0/V_J)/\varphi P_0$)); and (4) the flux of energy dissipated in processes other than trapping per active PSII (DI_0/RC). All calculations were performed using the instrument's software. Fluorescence data were pre-processed using the analytical tools available at CyanoTools (https://www.cyano.tools/OJIP_data_analysis).

Results

DIC images of planktonic and biofilm cultures: To investigate how planktonic *vs*. biofilm growth influences the structural organization of *Synechocystis* cells, we first compared DIC microscopic images of cultures grown in planktonic form to those of biofilm cultures (Fig. 1). Planktonic cultures existed as highly dispersed cell suspensions, containing only single cells and microcolonies (Fig. 1A, C). In contrast, biofilm cultures exhibited a significantly different appearance, characterized by a large number of cell aggregates with significant heterogeneity (Fig. 1B). Higher magnification (Fig. 1D) showed that intact cells were organized into compact, highly packed aggregates containing hundreds of cells. This tight spatial arrangement suggests strong cell-to-cell interactions and stable adhesion. In biofilm cultures, the aggregates ranged from small microcolonies of a few cells to large, compact clusters, suggesting that the physiological conditions inducing biofilm formation also promote cell-to-cell adhesion and colony development. Thus, the presented images represent two distinct physiological states: a planktonic lifestyle characterized by single cells and microcolonies and a biofilm-forming, aggregated lifestyle.

Effect of light intensity on biofilm aggregates

We determined the area of a significant number of individual aggregates (200–600) formed under different PFDs (10–400 µmol photons m^{-2} s^{-1}) to explore how light intensity affects the development and aggregate size distribution of the biofilm. The resulting distributions showed clear differences between treatments (Fig. 2A). The cumulative distribution function (CDF) curves under low-to-moderate light intensities (10–100 µmol photons m^{-2} s^{-1}) showed the dominance of small aggregates and only minor aggregate development. In contrast, a pronounced shift occurred at higher PFDs (250–400 µmol photons m^{-2} s^{-1}), indicating the formation of larger aggregates (Fig. 2A).

This structural shift was supported by the corresponding values of the log-normal distribution parameters, µ and σ (Supplementary Fig. 1A). Both parameters showed a similar pattern, with a minimum between 25 and 50 µmol photons m^{-2} s^{-1} PFD, and a strong increase above 100 µmol photons m^{-2} s^{-1} growth light intensity. The increase in both µ (mean area) and σ (distribution broadening) reflects a shift toward larger aggregates.

The magnitude of these changes is best demonstrated by the calculated mean aggregate areas (Fig. 2B). These data revealed small aggregate sizes (~ 15–20 μm^2) with only minor fluctuations between 10 and 100 µmol photons m^{-2} s^{-1} growth light intensities, followed by an increased up to 35 and 42 μm^2 under 250 and 400 µmol photons m^{-2} s^{-1} PFDs, respectively. This suggests that *Synechocystis* aggregate formation is enhanced by high irradiance.

Cultivation wavelength influences biofilm formation in Synechocystis

Compared to growth light intensity, cultivation wavelength influences aggregate size to a greater extent. *Synechocystis* cultures grown under monochromatic light showed a strong spectral dependence with regard to aggregate size distribution (Fig. 2C). Biofilm cultures grown under violet-to-green light (430–540 nm) were characterized by slowly rising CDF curves (with the most pronounced effect at 460–510 nm) compared to those of cultures grown under longer wavelengths. This indicates the formation of larger aggregates with remarkable size heterogeneity under violet-to-green light.

Accordingly, both μ and σ parameters (Supplementary Fig. 1B) and the mean area (Fig. 2D) peaked sharply at 460–510 nm. This indicates that cultivation under blue-green promotes not only an increase in aggregate size (~ 45–50 μm²) but also a robust broadening of the size distribution, resulting in a heterogeneous mixture of small to very large aggregates. Similar to the mean area, the μ and σ parameters had the lowest values at 560 nm, corresponding to uniformly small (~ 12 μm²) and narrowly distributed aggregates.

Light quantity and spectral quality strongly determine EPS production in Synechocystis

We determined the total polysaccharide content in cultures as a proxy for the polysaccharide-rich EPS level to investigate how light regimes (i.e., different light intensities and cultivation wavelengths) affect the secretion of EPS in *Synechocystis* (Fig. 3). EPS concentrations were significantly higher in biofilm cultures (~ 1–3 μg/mL) compared to planktonic ones (< 1 μg/mL), confirming that EPS secretion is closely related to cellular adhesion.

Over the applied PFD range, the EPS concentration of biofilm cultures showed a minimum under a 25 μmol photons m^{-2} s^{-1} growth light (Fig. 3A, black), in good accordance with the observation that this culture produced the smallest and least heterogeneous aggregates (Fig. 2A, B). At lower and higher PFDs, the EPS concentration was higher, reaching its maximum (~ 3 μg/mL) in cultures grown under white light with an intensity of 400 μmol photons m^{-2} s^{-1}. EPS concentration in planktonic cultures remained low across all studied light intensities (Fig. 3A, red), suggesting that EPS excretion is closely related to the biofilm-associated lifestyle rather than being a bulk cellular property. This contrasts with growth rates, which are substantially higher in planktonic cultures than in biofilms.

EPS production in *Synechocystis* biofilm cultures was more sensitive to cultivation wavelength than to light intensity (Fig. 3B). Under a constant PFD of 25 μmol photons m^{-2} s^{-1}, violet-to-green monochromatic illumination (430–540 nm) induced the highest EPS levels (~ 3–7 μg/mL), which were remarkably higher than those under all other wavelengths (~ 0.5–1.5 μg/mL). The EPS content reached its minimum values (~ 0.5 μg/mL), comparably to planktonic levels (Fig. 3A), under yellow-orange wavelengths (560–590 nm). This wavelength dependence is very similar to that of aggregate size (Fig. 2D), indicating that blue light promotes EPS biosynthesis and, in turn, increases aggregate size and heterogeneity.

EPS production and aggregate formation under a changing light regime

Figure 4 shows how EPS production responds to a changing light regime. During pre-cultivation under warm-white light (A) and, subsequently, under red (630 nm) cultivation light (B), the EPS content stayed low (~ 1 µg/mL) with a concomitantly small mean aggregate area (< 20 µm²). However, upon transfer to 460 nm light (C), the EPS concentration increased rapidly and continuously, reaching the highest value observed in our study. In parallel, the mean aggregate area increased from ~ 15 µm² to ~ 70 µm². The simultaneous increase in both parameters suggests a strong positive relationship between EPS accumulation and cell aggregation. Microscopic observations confirmed the appearance of larger and denser colonial structures during this phase. When cultures were shifted back to red light after a dilution (D, B'), the EPS concentration and aggregate size returned to their original levels. As previously shown (Zavřel et al. 2024), *Synechocystis* cultures grown under 630 nm and 460 nm lights exhibit the highest and lowest growth rates (Supplementary Table 1), respectively, among the nine tested wavelengths, the opposite of what we observed for EPS secretion. This suggests that EPS production is not a passive accompanying phenomenon of growth but rather an actively regulated photo-physiological response.

PSII photochemistry in planktonic and biofilm cells

Several chlorophyll fluorescence parameters (derived from OJIP curves; see Materials and Methods) were determined in both planktonic and biofilm *Synechocystis* cultures over a range of PFDs and nine monochromatic growth wavelengths (Fig. 5). These parameters were used to characterize PSII photochemistry, electron transport capacity, and energy dissipation in the cultures.

Effect of growth light intensity on PSII photochemistry (Fig. 5A-D). The light dependence of the normalized area above the OJIP transient (S_M) displayed entirely different patterns between the two growth modes (Fig. 5A). In planktonic cells, S_M reached a maximum at a PFD of 25 µmol photons m^{-2} s^{-1} and decreased gradually with increasing light intensities. In contrast, biofilm cells exhibited high S_M values only under a growth light of 10 µmol photons m^{-2} s^{-1}, while under other intensities, S_M values remained low. This indicates a reduced electron acceptor capacity in biofilm cultures under elevated irradiance.

The maximum quantum yield of PSII photochemistry decreased with increasing light intensities in both planktonic and biofilm cells (Fig. 5B). The obtained φP_0 values (~ 0.3–0.4) were statistically similar between the two life forms under low-to-moderate light intensities. However, biofilm cells showed significantly lower values (~ 0.12) compared to the planktonic ones (~ 0.22) at the highest applied irradiance. This suggests a more effective electron transport in planktonic *Synechocystis* cells than in biofilm ones under high light intensities.

This conclusion is well supported by DI_0/RC data. This flux of dissipated energy increased gradually in biofilm cells with increasing PFDs (Fig. 5C). However, while planktonic cells showed only a moderate increase and minor fluctuations, biofilm cells displayed a much steeper rise under high light intensities, indicating an enhanced energy dissipation under high light conditions.

The apparent antenna size per active PSII reaction center (ABS/RC) also increased with increasing PFDs in both planktonic and biofilm cells (Fig. 5D). However, biofilm cells showed higher ABS/RC values compared to planktonic ones at irradiances above 100 µmol photons m^{-2} s^{-1}. This difference became significant above 250 µmol photons m^{-2} s^{-1}, indicating a higher absorption cross-section per active reaction center in the biofilm cultures.

Effect of growth light wavelength on PSII photochemistry (Fig. 5E-H). The highest S_M values were observed in the blue-green region (430–540 nm) in biofilm cells, whereas planktonic cells exhibited maximum S_M values at longer wavelengths, around 590–660 nm (Fig. 5E).

The φP_0 values showed a strong wavelength dependence (Fig. 5F) in both cultures. Biofilm cells maintained relatively high φP_0 values in the violet-green region (430–530 nm) and near far-red light (690 nm), reaching 0.50–0.53. In contrast, planktonic cells exhibited a pronounced decrease in φP_0 under blue-green wavelengths, with minimum values around 0.20–0.25, followed by a recovery at longer wavelengths. Thus, biofilm cells appeared considerably less sensitive to blue-light stress than planktonic cells.

The parameters DI_0/RC and ABS/RC exhibited nearly identical trends (Fig. 5G–H). In planktonic cultures, both parameters showed peak values around 460–510 nm, indicating enhanced energy dissipation and larger apparent antenna sizes under blue-green light. Biofilm cells showed much lower values within this spectral region and remained relatively stable across most wavelengths. DI_0/RC and ABS/RC values declined in biofilm cells but remained relatively high in planktonic cultures at 690 nm.

Discussion

Our results with planktonic and biofilm *Synechocystis* cultures showed a light-dependent, reversible transition from unicellular organization to a biofilm lifestyle. While planktonic cultures were predominantly unicellular, biofilm cultures consisted of aggregates with a broad spectrum of size distribution, ranging from microcolonies comprising a few cells to large, compact clusters. Aggregate formation suggests that *Synechocystis* cells in a biofilm switched to a physiological state that promotes cell-to-cell adhesion and matrix formation, rather than representing passive sedimentation or a surface-associated phenomenon (Fisher et al., 2013; Jittawuttipoka et al., 2013; Enomoto et al., 2015). Biofilm-associated aggregation has been described previously in *Synechocystis* and other cyanobacteria. The observed aggregation is a consequence of an enhanced EPS production, which changes cell surface properties and, in turn, increases cellular adhesive capacity (Fisher et al., 2013; Enomoto et al. 2015). The transition from unicellular to colonial organization has also been observed in *Microcystis*, *Nostoc*, and *Anabaena* species, where aggregation provides a distinct advantage by enhancing stress tolerance and environmental resistance (De Philippis et al., 2001; Gan et al., 2012; Sand-Jensen, 2014). Our observations based on microscopic imaging (Fig. 1) and subsequent quantitative analyses of aggregate size (Fig. 2), as well as the determined EPS levels (Figs. 3, 4) and photosynthetic parameters (Fig. 5) clearly confirm that the biofilm lifestyle fundamentally differs from the planktonic counterpart.

The observed structural differences were correlated with the transition from a planktonic to a biofilm lifestyle (Fig. 1). The absence of large aggregates in planktonic cultures (Fig. 1A, C) suggested that under these conditions, the cells remained freely suspended, whereas biofilm cultures (Fig. 1B, D) exhibited a pronounced colonial organization. Colonial organization may contribute to altered physiological properties, including modified diffusion gradients, increased resistance to environmental stress, and changes in photosynthetic performance compared to planktonic cells. Physiological heterogeneity has been reported in cyanobacterial mats formed by filamentous genera such as *Microcoleus*, *Oscillatoria*, and *Phormidium*, where chemical and light gradients drive the spatial differentiation in metabolism (Jo et al., 2022; Stewart et al., 2008). In the wild-type *Synechocystis* sp. PCC 6803, aggregation and biofilm formation have been associated with cell-surface structures and EPS secretion that evolved stable colonial assemblies (Allen et al., 2019).

Quantitative analysis of the size distribution of cellular clusters revealed that light intensity significantly influences the size and heterogeneity of *Synechocystis* aggregates (Fig. 2A, B). Under moderate PFDs, *Synechocystis* biofilms are dominated by relatively small, narrowly distributed aggregates, whereas low and high PFDs induce the formation of larger clusters with greater structural heterogeneity. In cyanobacterial biofilms, EPS production is essential for cell-to-cell adhesion, as well as aggregate development and expansion (De Philippis et al., 1998; Seminara et al., 2012). The similarity between the light-intensity dependence of aggregate size (Fig. 2B) and EPS secretion (Fig. 3A) confirms that both low and, in particular, high irradiance facilitate EPS-mediated cellular adhesion. A sub-optimal light environment may trigger protective responses, including increased production of EPS, which can act as a physical barrier between the cell surface and the environment, as well as the appearance of larger, heterogeneous aggregates (at higher PFDs) to protect cells against photodamage *via* self-shading (Pereira et al., 2009; Rossi and De Philippis, 2015).

Compared to light intensity, growth wavelength had an even more pronounced influence on aggregate size and heterogeneity in *Synechocystis* biofilms (Fig. 2C, D). Blue and blue-green growth lights induce the formation of remarkably large, heterogeneous aggregates, whereas growth under yellow-orange light promotes the formation of uniformly small structures, similar to those in planktonic cultures. Growth under near-far-red light (690 nm) resulted in intermediate aggregation. This wavelength-dependent phenomenon strongly suggests the involvement of blue-light-specific signaling pathways rather than energetic effects. In *Synechocystis*, several blue-light photoreceptors and cryptochrome-like proteins regulate cellular behavior, including phototaxis, type IV pili-dependent motility, stress responses, and gene expression (Masuda and Bauer, 2002; Song et al., 2011; Wiltbank and Kehoe, 2019; Sugimoto et al., 2017). In cyanobacteria and other phototrophs, blue light enhances EPS accumulation and cellular-surface attachment, often independently of the growth rate (Ikeuchi and Ishizuka, 2008; Enomoto et al., 2015).

The strong wavelength dependence of aggregate dynamics (Fig. 2C, D) correlates well with that of EPS production (Fig. 3B). Based on research by Luimstra et al. (2018), blue light (~ 450 nm) has a significant negative effect on the growth of *Synechocystis* cells compared to red or white light. Blue light triggers

extracellular matrix formation, creating a physical barrier to protect cells against excess excitation energy within the heterogeneous biofilm structures. In contrast, orange-red light is effectively absorbed and utilized by *Synechocystis*, promoting rapid growth (Zavřel et al., 2024) and low EPS production. This induces a planktonic-like physiological state, since under optimal conditions, protection and biofilm formation are unnecessary.

The EPS secretion and aggregate formation in biofilm cultures change dynamically, depending on the light regime. EPS determination under changing environmental (light) conditions (Fig. 4) demonstrates that EPS production in biofilm cultures is actively regulated (De Philippis et al., 2001; Ehling-Schulz et al., 1997). The parallel increase of EPS concentration and aggregate size suggests that extracellular polysaccharides play a central role in mediating cell-to-cell adhesion and aggregate stability. Upon switching from red to blue growth light, cellular growth significantly slowed down, accompanied by an enhanced EPS concentration (Zavřel et al., 2024, this work). This completely opposite wavelength dependence of cell growth and EPS secretion suggests that the latter is an active regulatory process, rather than a passive secretion driven by cell proliferation (Gan et al., 2012.; Otero and Vincenzini, 2003). Similar inverse effects were found also in *Nostoc sp.* and *Microcystis sp.* strains, where EPS production increased under stress or sub-optimal growth conditions (De Philippis et al., 2001; Gan et al., 2012). The decrease in EPS concentration and aggregate size after dilution and switching from blue to red light demonstrates that the aggregated state is dynamic and dependent on both cell density and continued environmental stimulation. This reversibility suggests a remarkable physiological plasticity of *Synechocystis* cells under changing environmental conditions. Overall, the data support a model in which blue light is one of the key environmental signals contributing to EPS synthesis and colonial organization in *Synechocystis*. The increased EPS accumulation observed in the GT-L strain under blue light most likely reflects the enhanced synthesis of released and/or cell-associated polysaccharides (Santos et al., 2021) that contribute to cellular aggregation and biofilm matrix formation.

Biofilm-associated cells showed a reduced pool size of electron acceptors (S_M) over almost the entire range of light intensities (Fig. 5A), as well as a lower maximum photochemical efficiency (φP_0), enhanced energy dissipation (DI_0/RC), and an enlarged apparent antenna size (ABS/RC) under high light compared to planktonic cells (Fig. 5B–D). All of these changes are characteristic of photoprotective acclimation (Strasser et al., 2004; Campbell et al., 1998; Hendrickson et al., 2005). The concomitant increase in ABS/RC and DI_0/RC suggests that the higher excitation pressure per active PSII is compensated for by an enhanced dissipation of excess energy as heat or fluorescence (Al-Najjar et al., 2010) in biofilm cells. Reduced S_M values further indicate a limitation on downstream electron transport, which may serve to prevent over-reduction of the photosynthetic electron transport chain (especially the plastoquinone pool) under higher light (Strasser et al., 2004). These photochemical features concur with the conditions promoting large aggregate formation and EPS accumulation (Figs. 2, 3). Biofilms and mats modify the local light environment *via* light scattering and absorption, potentially increasing excitation heterogeneity within aggregates (Kühl, 2005; Al-Najjar et al., 2010).

The biofilm-associated cells showed a distinct spectral response compared with planktonic cells (Fig. 5E-H). The high φP_0 values (Fig. 5F) and relatively low DI_0/RC (Fig. 5G) under blue light suggest that biofilm cells are better adapted to utilize blue wavelengths while avoiding excessive excitation pressure. This finding is consistent with the enhanced EPS production (Figs. 3B, 4) and aggregation (Figs. 2D, 4) observed under blue-light cultivation, indicating that blue light may induce a coordinated physiological state involving both biofilm development and photosynthetic acclimation (Scott et al. 2006; Luimstra et al., 2018; Zavřel et al. 2024). The elevated DI_0/RC and ABS/RC (Fig. 5G, H) values observed in planktonic cells under blue-green light indicate increased excitation stress and enhanced thermal energy dissipation. In contrast, the more stable response of biofilm cells suggests that the biofilm matrix may buffer the rapid fluctuations in the light environment, reducing the need for excessive energy dissipation. Self-shading, altered pigment composition (Kubushiro et al., 2025), and modified electron transport capacity in the cell-aggregates may all contribute to this enhanced tolerance. Overall, biofilm and planktonic *Synechocystis* cells exhibit fundamentally different photosynthetic acclimation strategies based on OJIP analysis. Biofilm cells show enhanced photoprotective capacity (Kühl et al., 1996; Rossi and De Philippis, 2015) and greater plasticity to spectral dependent changes, whereas planktonic cells are more strongly affected by blue-light excitation and high-irradiance stress.

Our results demonstrate that both light quantity and quality strongly influence aggregate formation, EPS production, and photosynthetic efficiency in *Synechocystis* sp. PCC 6803 GT-L. This coordinated performance highlights the close interrelationship between cellular growth and protection, which is critical for survival in ever-changing aquatic and benthic environments. The light-dependent reversible transition between planktonic and biofilm lifestyles observed in *Synechocystis* shows how environmental signals can regulate colonial organization, thereby enhancing the ecological fitness and long-term persistence of cyanobacterial populations in dynamic habitats. The obtained data provide a deeper insight into cyanobacterial ecology and have potential relevance for various biotechnological applications including biofilm engineering.

Declarations

Declaration of competing interest

The authors declare that they have no known competing financial interests or personal relationships that could have appeared to influence the work reported in this paper.

Author contribution statement

MK designed the experiments. MK and AWK performed experiments. MK analysed the results. MK and GB wrote the manuscript. All authors reviewed, revised, and approved the final manuscript for publication.

Funding

This work was supported by the National Multidisciplinary Laboratory for Climate Change (RRF-2.3.1-21-2022-00014) project, implemented within the framework of Hungary's National Recovery and Resilience Plan, and funded by the Recovery and Resilience Facility of the European Union.

Author Contribution

MK designed the experiments. MK and AWK performed experiments. MK analysed the results. MK and GB wrote the manuscript. All authors reviewed, revised, and approved the final manuscript for publication.

Data availability statement

All data and material are available upon request of the corresponding author. Additionally, we provide a freely accessible online tool for streamlined processing and preliminary analysis of fluorescence data from kinetic fluorometers and spectrofluorometers used in this study, available at https://www.cyano.tools/OJIP_data_analysis.

References

1. Al-Najjar M, de Beer D, Jørgensen B, Kühl M, Polerecky L (2010) Conversion and conservation of light energy in a photosynthetic microbial mat ecosystem. ISME J 4:440–449. https://doi.org/10.1038/ismej.2009.121
2. Allen R, Rittmann BE, Curtiss R III (2019) Axenic biofilm formation and aggregation by *Synechocystis* sp. strain PCC 6803 are induced by changes in nutrient concentration and require cell surface structures. Appl Environ Microbiol 85(7):e02192–e02118. https://doi.org/10.1128/AEM.02192-18
3. Bernát G, Zavřel T, Kotabová E, Kovács L, Steinbach G, Vörös L, Prášil O, Somogyi B, Tóth VR (2021) Photomorphogenesis in the Picocyanobacterium *Cyanobium gracile* Includes Increased Phycobilisome Abundance Under Blue Light, Phycobilisome Decoupling Under Near Far-Red Light, and Wavelength-Specific Photoprotective Strategies. Front Plant Sci 12:612302. 10.3389/fpls.2021.612302
4. Bhaya D, Bianco NR, Bryant D, Grossman A (2002) Type IV pilus biogenesis and motility in the cyanobacterium *Synechocystis* sp. PCC6803. Mol Microbiol 37:941–951. https://doi.org/10.1046/j.1365-2958.2000.02068.x
5. Burnap RL, Hagemann M, Kaplan A (2015) Regulation of CO_2 concentrating mechanisms in cyanobacteria. Life 5:348–371. https://doi.org/10.3390/life5010348
6. Campbell D, Hurry V, Clarke AK, Gustafsson P, Öquist G (1998) Chlorophyll fluorescence analysis of cyanobacterial photosynthesis and acclimation. Microbiol Mol Biol Rev 62(3):667–683.

10.1128/MMBR.62.3.667-683.1998

7. Chen Z, Li X, Tan X, Zhang Y, Wang B (2020) Recent Advances in Biological Functions of Thick Pili in the Cyanobacterium Synechocystis sp. PCC 6803. Front Plant Sci 11:241. https://doi.org/10.3389/fpls.2020.00241
8. Costerton JW, Lewandowski Z, Caldwell DE, Korber DR, Lappin-Scott HM (1995) Microbial biofilms. Annu Rev Microbiol 49:711–745. https://doi.org/10.1146/annurev.mi.49.100195.003431
9. de Beer D, Stoodley P, Roe F, Lewandowski Z (1997) Effects of biofilm structures on oxygen distribution and mass transport. Biotechnol Bioeng 43(11):1131–1138. 10.1002/bit.260431118
10. De Philippis R, Vincenzini M (1998) Exocellular polysaccharides from cyanobacteria and their possible applications. FEMS Microbiol Rev 22:151–175. https://doi.org/10.1111/j.1574-6976.1998.tb00365.x
11. De Philippis R, Sili C, Paperi R, Vincenzini M (2001) Exopolysaccharide-producing cyanobacteria and their possible exploitation: a review. J Appl Phycol 13:293–299. https://doi.org/10.1023/A:1017590425924
12. DuBois M, Gilles KA, Hamilton JK, Rebers PA, Smith F (1956) Colorimetric method for determination of sugars and related substances. Anal Chem 28(3):350–356. https://doi.org/10.1021/ac60111a017
13. Ehling-Schulz M, Bilger W, Scherer S (1997) UV-B-induced synthesis of photoprotective pigments and extracellular polysaccharides in the terrestrial cyanobacterium *Nostoc commune*. J Bacteriol 179:1940–1945. 10.1128/jb.179.6.1940-1945.1997
14. Enomoto G, Nomura R, Shimada T, Ni-Ni-Win, Narikawa R, Ikeuchi M (2014) Cyanobacteriochrome SesA is a diguanylate cyclase that induces cell aggregation in *Thermosynechococcus*. J Biol Chem 289(36):24801–24809. 10.1074/jbc.M114.583674
15. Enomoto G, Ni-Ni-Win, Narikawa R, Ikeuchi M (2015) Three cyanobacteriochromes work together to form a light colour-sensitive input system for c-di-GMP signalling of cell aggregation. *Proceedings of the National Academy of Sciences USA*, 112(26), 8082–8087. 10.1073/pnas.1504228112
16. Fisher ML, Allen R, Luo Y, Curtiss R III (2013) Export of extracellular polysaccharides modulates adherence of the cyanobacterium *Synechocystis*. PLoS ONE 8(9):e74514. https://doi.org/10.1371/journal.pone.0074514
17. Flemming H-C, Wingender J (2010) The biofilm matrix. Nat Rev Microbiol 8:623–633. https://doi.org/10.1038/nrmicro2415
18. Gan N, Xiao Y, Zhu L, Wu Z, Liu J, Hu C, Song L (2012) The role of microcystins in maintaining colonies of bloom-forming *Microcystis* spp. Environ Microbiol 14(3):730–742. https://doi.org/10.1111/j.1462-2920.2011.02624.x
19. Gan F, Zhang S, Rockwell NC, Martin SS, Lagarias JC, Bryant DA (2014) Extensive remodeling of a cyanobacterial photosynthetic apparatus in far-red light. Science 345:1312–1317. https://doi.org/10.1126/science.1256963

20. Hagemann M, Hess WR (2018) Systems and synthetic biology for the biotechnological application of cyanobacteria. Curr Opin Biotechnol 49:94–99. https://doi.org/10.1016/j.copbio.2017.07.008
21. Helbling EW, Banaszak AT, Villafañe VE (2015) Global change feed-back inhibits cyanobacterial photosynthesis. Sci Rep 5:14514. https://doi.org/10.1038/srep14514
22. Hendrickson L, Forster B, Pogson BJ, Chow WS (2005) A simple chlorophyll fluorescence parameter that correlates with the rate coefficient of photoinactivation of Photosystem II. Photosynth Res 84(1–3):43–49. https://doi.org/10.1007/s11120-004-6430-4
23. Hihara Y, Sonoike K, Kanehisa M, Ikeuchi M (2003) DNA microarray analysis of redox-responsive genes in the genome of the cyanobacterium Synechocystis sp. strain PCC 6803. J Bacteriol 185(5):1719–1725. 10.1128/JB.185.5.1719-1725.2003
24. Hirano SS, Nordheim EV, Arny DC, Upper CD (1982) Lognormal Distribution of Epiphytic Bacterial Populations on Leaf Surfaces. Appl Environ Microbiol 44(3). https://doi.org/10.1128/aem.44.3.695-700.1982
25. Ikeuchi M, Tabata S (2001) Synechocystis sp. PCC 6803—A useful tool in the study of the genetics of cyanobacteria. Photosynth Res 70:73–83. 10.1023/A:1013887908680
26. Ikeuchi M, Ishizuka T (2008) Cyanobacteriochromes: a new superfamily of tetrapyrrole-binding photoreceptors in cyanobacteria. Photochem Photobiol Sci 7:1159–1167. https://doi.org/10.1039/b802660m
27. Jittawuttipoka T, Planchon M, Spalla O, Benzerara K, Guyot F, Cassier-Chauvat C, Chauvat F (2013) Multidisciplinary evidence that *Synechocystis* PCC 6803 exopolysaccharides operate in cell sedimentation and protection against salt and metal stresses. PLoS ONE 8(2):e55564. https://doi.org/10.1371/journal.pone.0055564
28. Jo J, Price-Whelan A, Dietrich LEP (2022) Gradients and consequences of heterogeneity in biofilms. Nat Rev Microbiol 20:593–607. https://doi.org/10.1038/s41579-022-00692-2
29. Kaneko T, Sato S, Kotani H, Tanaka A, Asamizu E, Nakamura Y, Miyajima N, Hirosawa N, Sugiura M, Sasamoto S, Kimura T, Hosouchi T, Matsuno A, Muraki A, Nakazaki A, Naruo K, Okumura S, Shimpo S, Takeuchi C, Wada T, Watanabe T, Yamada M, Yasuda M, Tabata S (1996) Sequence analysis of the genome of the unicellular cyanobacterium *Synechocystis* sp. PCC 6803. DNA Res 3:109–136. https://doi.org/10.1093/dnares/3.3.109
30. Koskinen S, Kurkela J, Linhartová M, Tyystjärvi T (2023) The genome sequence of Synechocystis sp. PCC 6803 substrain GT-T and its implications for the evolution of PCC 6803 substrains. FEBS Open Bio 4701–712. 10.1002/2211-5463.13576
31. Keithley SE, Kirisits MJ (2018) An improved protocol for extracting extracellular polymeric substances from granular filter media. Water Res 129:419–427. https://doi.org/10.1016/j.watres.2017.11.020
32. Kis M, Sipka G, Ayaydin F, Maróti P (2018) The biophysics of a critical phenomenon: colonization and sedimentation of the photosynthetic bacteria *Rubrivivax gelatinosus*. Eur Biophys J 47:139–149. https://doi.org/10.1007/s00249-017-1236-4

33. Kis M, Zavřel T, Fodor I (2026) Low PSI content broadens the optimal light spectrum for a phycoerythrin-dominated cyanobacterium towards near far-red. Sci Rep. https://doi.org/10.1038/s41598-026-50772-z
34. Kubushiro M, Otsu T, Misawa N, Hamada M, Eki T, Kawai S, Hirose Y (2025) Partial photoswitching of rod-shaped phycobilisome production in the cyanobacterium Synechocystis sp. PCC 6803. Plant Cell Physiol 66:1274–1283. 10.1093/pcp/pcaf064
35. Kühl M, Lassen C, Jørgensen BB (1994) Light penetration and light intensity in sandy marine sediments measured with irradiance and scalar irradiance fiber-optic microprobes. Mar Ecol Prog Ser 105:139–148. https://doi.org/10.3354/meps105139
36. Kühl M et al (1996) Microenvironmental control of photosynthesis in an epilithic cyanobacterial biofilm. J Phycol 32:799–812. https://doi.org/10.1111/j.0022-3646.1996.00799.x
37. Kühl M (2005) Optical microsensors for analysis of microbial communities. Methods Enzymol 397:166–199. https://doi.org/10.1016/S0076-6879(05)97010-9
38. Luimstra VM, Schuurmans JM, Verschoor AM, Hellingwerf KJ, Huisman J, Matthijs HCP (2018) Blue light reduces photosynthetic efficiency of cyanobacteria through an imbalance between photosystems I and II. Photosynth Res 138(2):177–189. 10.1007/s11120-018-0561-5
39. Maeda K, Okuda Y, Enomoto G, Watanabe S, Ikeuchi M (2021) Biosynthesis of a sulfated exopolysaccharide, synechan, and bloom formation in the model cyanobacterium *Synechocystis* sp. PCC 6803. *eLife*, 10, e66538. https://doi.org/10.7554/eLife.66538
40. Masuda S, Bauer CE (2002) AppA is a blue-light photoreceptor that antirepresses photosynthesis gene expression in *Rhodobacter sphaeroides*. Cell 110(5):613–623. https://doi.org/10.1016/S0092-8674(02)00876-0
41. Murata N, Takahashi S, Nishiyama Y, Allakhverdiev SI (2007) Photoinhibition of photosystem II under environmental stress. Biochim Biophys Acta 1767:414–421. https://doi.org/10.1016/j.bbabio.2006.11.019
42. Otero A, Vincenzini M (2003) Extracellular polysaccharide synthesis by *Nostoc* strains as affected by N source and light intensity. J Biotechnol 102:143–152. https://doi.org/10.1016/S0168-1656(03)00022-1
43. Paerl HW, Pinckney JL (1996) A mini-review of microbial consortia: their roles in aquatic production and biogeochemical cycling. Microb Ecol 31:225–247. https://doi.org/10.1007/BF00171569
44. Pereira S, Zille A, Micheletti E, Moradas-Ferreira P, De Philippis R, Tamagnini P (2009) Complexity of cyanobacterial exopolysaccharides: composition, structures, inducing factors and putative genes. FEMS Microbiol Rev 33(5):917–941. https://doi.org/10.1111/j.1574-6976.2009.00183.x
45. Pereira SB, Mota R, Vieira CP, Vieira J, Tamagnini P, De Philippis R (2015) Phylum-wide analysis of genes related to the assembly and export of extracellular polymeric substances in cyanobacteria. Sci Rep 5:14835. https://doi.org/10.1038/srep14835
46. Rochex A, Lebeault JM (2007) Effects of nutrients on biofilm formation and detachment of a *Pseudomonas putida* strain isolated from a paper machine. Water Res 41(13):2885–2892.

https://doi.org/10.1016/j.watres.2007.03.041

47. Rossi F, De Philippis R (2015) Role of cyanobacterial exopolysaccharides in phototrophic biofilms and in complex microbial mats. Life (Basel) 5(2):1218–1238. 10.3390/life5021218
48. Santos M, Pereira SB, Flores C, Príncipe C, Couto N, Karunakaran E, Cravo SM, Oliveira P, Tamagnini P (2021) Absence of KpsM (Slr0977) Impairs the Secretion of Extracellular Polymeric Substances (EPS) and Impacts Carbon Fluxes in *Synechocystis* sp. PCC 6803. mSphere. 6(1):e00003–21. 10.1128/mSphere.00003-21
49. Schindelin J, Arganda-Carreras I, Frise E, Kaynig V, Longair M, Pietzsch T, Preibisch S, Rueden C, Saalfeld S, Schmid B, Tinevez JY, White DJ, Hartenstein V, Eliceiri K, Tomancak P, Cardona A (2012) Fiji: an open-source platform for biological-image analysis. Nat Methods 9(7) 676 – 82. https://doi:10.1038/nmeth.2019
50. Scott M, McCollum C, Vasil'ev S et al (2006) Mechanism of the down regulation of photosynthesis by blue light in the cyanobacterium Synechocystis sp. PCC 6803. Biochemistry 45:8952–8958. 10.1021/bi060767p
51. Song J-Y, Cho H-S, Cho J-I, Jeon J-S, Lagarias JC, Park Y-I (2011) Near-UV cyanobacteriochrome signaling system elicits negative phototaxis in the cyanobacterium *Synechocystis* sp. PCC 6803. Proc Natl Acad Sci USA 108(26):10780–10785. https://doi.org/10.1073/pnas.1104242108
52. Sugimoto Y, Nakamura H, Ren S, Hori K, Masuda S (2017) Genetics of the Blue Light-Dependent Signal Cascade That Controls Phototaxis in the Cyanobacterium *Synechocystis* sp. PCC6803. Plant Cell Physiol 58(3):458–465. https://doi.org/10.1093/pcp/pcw218
53. Stal LJ (1995) Physiology of cyanobacteria in microbial mats and other communities. New Phytol 131:1–32. https://doi.org/10.1111/j.1469-8137.1995.tb03051.x
54. Stanier RY, Kunisawa R, Mandel M, Cohen-Bazire G (1971) Purification and properties of unicellular blue-green algae (order Chroococcales). Bacteriol Reviews 35:171–205. 10.1128/br.35.2.171-205.1971
55. Strasser RJ, Tsimilli-Michael M, Srivastava A (2004) Analysis of the chlorophyll a fluorescence transient. In: Papageorgiou GC, Govindjee (eds) Chlorophyll a Fluorescence: A Signature of Photosynthesis. Advances in Photosynthesis and Respiration, vol 19. Springer, Dordrecht, pp 321–362. https://doi.org/10.1007/978-1-4020-3218-9_12
56. Stewart P, Franklin M (2008) Physiological heterogeneity in biofilms. Nat Rev Microbiol 6:199–210. https://doi.org/10.1038/nrmicro1838
57. Tamaru Y, Takani Y, Yoshida T, Sakamoto T (2005) Crucial role of extracellular polysaccharides in desiccation and freezing tolerance in the terrestrial cyanobacterium *Nostoc commune*. Appl Environ Microbiol 71:7327–7333. https://doi.org/10.1128/AEM.71.11.7327-7333.2005
58. Tsagkari E, Connelly S, Liu Z et al (2022) The role of shear dynamics in biofilm formation. npj Biofilms Microbiomes 8:33. https://doi.org/10.1038/s41522-022-00300-4
59. Whitton BA, Potts M (2012) Ecology of Cyanobacteria II: Their Diversity in Space and Time. Springer, Dordrecht. https://doi.org/10.1007/978-94-007-3855-3

60. Wilking JN, Angelini TE, Seminara A, Brenner MP, Weitz DA (2011) Biofilms as complex fluids. MRS Bull 36:385–391. https://doi.org/10.1557/mrs.2011.71
61. Wiltbank LB, Kehoe DM (2019) Diverse light responses of cyanobacteria mediated by phytochrome-superfamily photoreceptors. Nat Rev Microbiol 17:37–50. https://doi.org/10.1038/s41579-018-0110-4
62. Zavřel T, Sinetova MA, Búzová D, Literáková P, Červený J (2015) Characterization of a model cyanobacterium Synechocystis sp. PCC 6803 autotrophic growth in a flat-panel photobioreactor. Eng Life Sci 15:122–132
63. Tomáš Zavřel,Petra Očenášová, Jan Červený (2017) Phenotypic characterization of *Synechocystis* sp. PCC 6803 substrains reveals differences in sensitivity to abiotic stress. PLoS ONE. https://doi.org/10.1371/journal.pone.0189130
64. Zavřel T, Segečová A, Kovács L, Lukeš M, Novák Z, Pohland A-C, Szabó M, Somogyi B, Prášil O, Červený J, Bernát G (2024) A Comprehensive Study of Light Quality Acclimation in *Synechocystis* Sp. PCC 6803. Plant Cell Physiol 65:1285–1297. https:/doi: 10.1093/pcp/pcae062

Figures

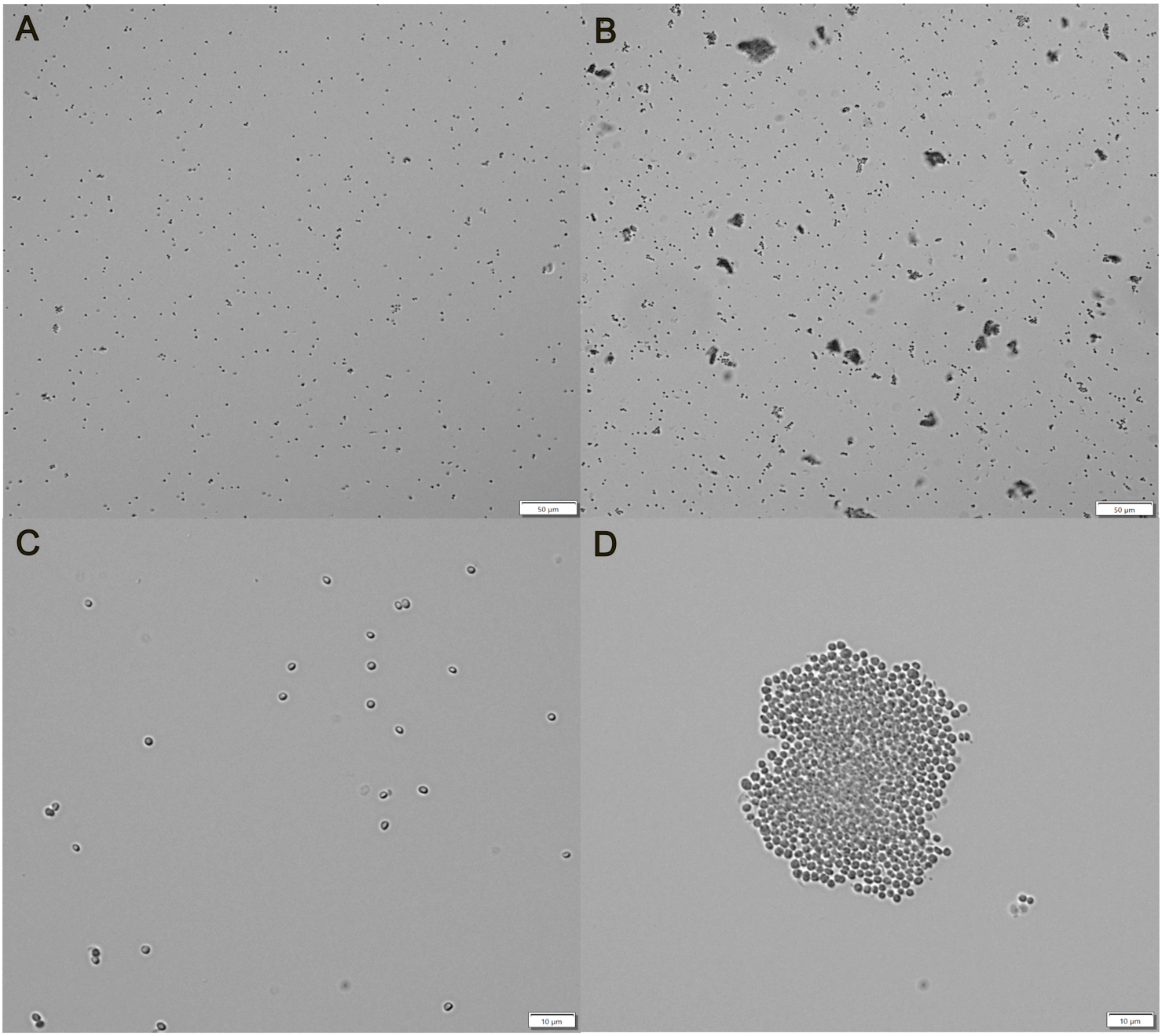


Figure 1

Differential interference contrast (DIC) micrographs of *Synechocystis* cultures grown in planktonic (A, C) or biofilm lifestyles (B, D). Scale bars: 50 µm (A, B) and 10 µm (C, D).

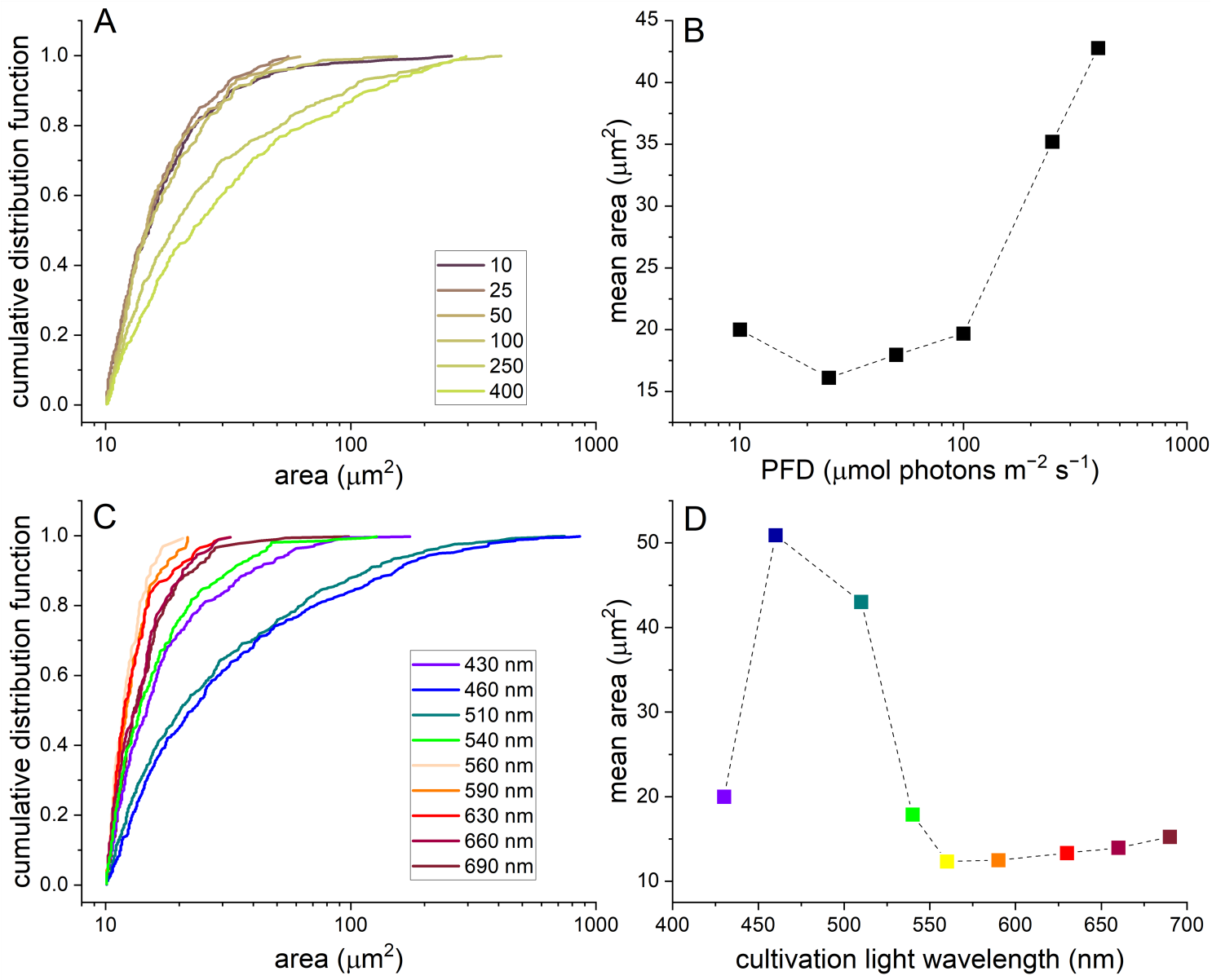


Figure 2

Log-normal size (area) distribution of *Synechocystis* biofilm aggregates developed under various photon flux densities (PFDs) (A, B) and nine different monochromatic lights (C, D). (A, C) Cumulative distribution function (CDF) curves of aggregate areas in biofilm cultures grown under various PFDs (10–400 μmol photons m^{-2} s^{-1}) or monochromatic lights (430-690 nm) at a constant PFD of 25 μmol photons m^{-2} s^{-1}, respectively. (B, D) Mean aggregate areas derived from the log-normal fits of cultures grown under various PFDs and monochromatic lights, respectively.

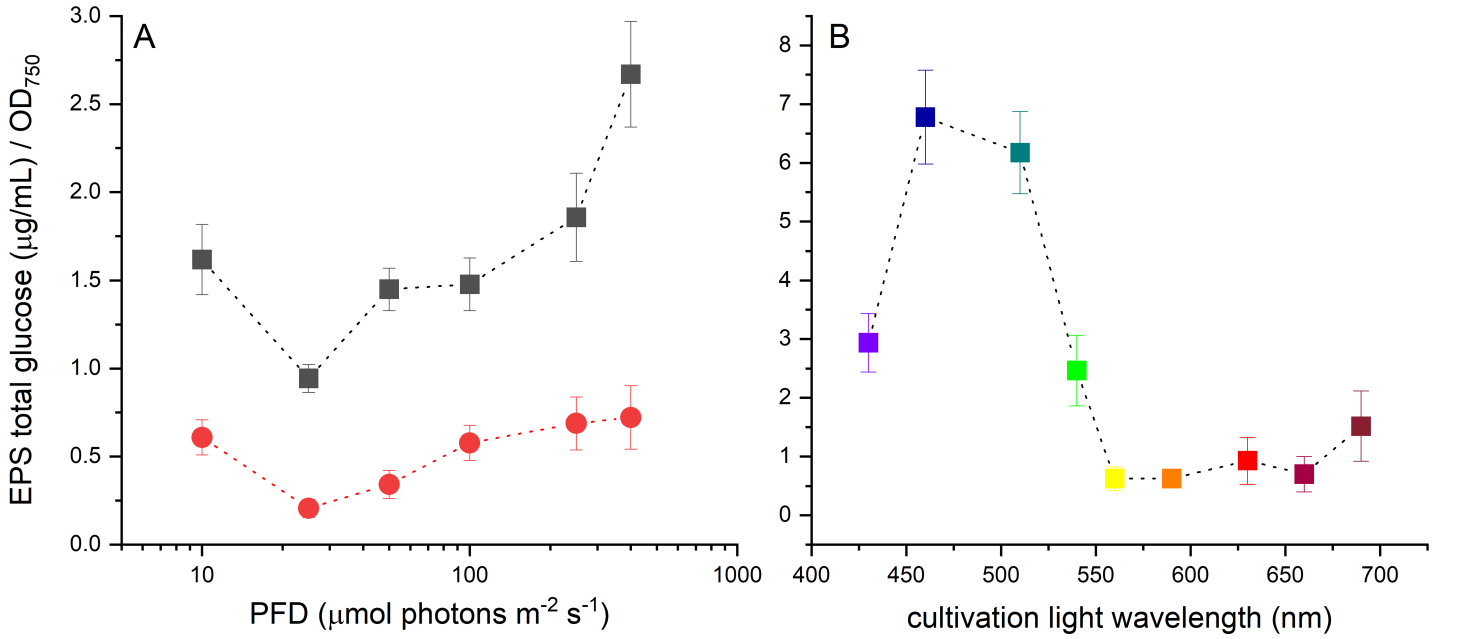


Figure 3

Extracellular polymeric substance (EPS) levels, determined as total glucose concentration normalized to biomass (OD_{750}), in *Synechocystis* planktonic (circles) and biofilm (squares) cultures grown under different light regimes. (A) EPS content as a function of PFD (10-400 µmol photons m^{-2} s^{-1}) and (B) EPS content as a function of growth wavelength (430-690 nm) at a constant PFD of 25 µmol photons m^{-2} s^{-1}. Total glucose equivalents are expressed in µg mL^{-1} OD_{750}^{-1}.The values represent the mean ± SD (n = 4–6).

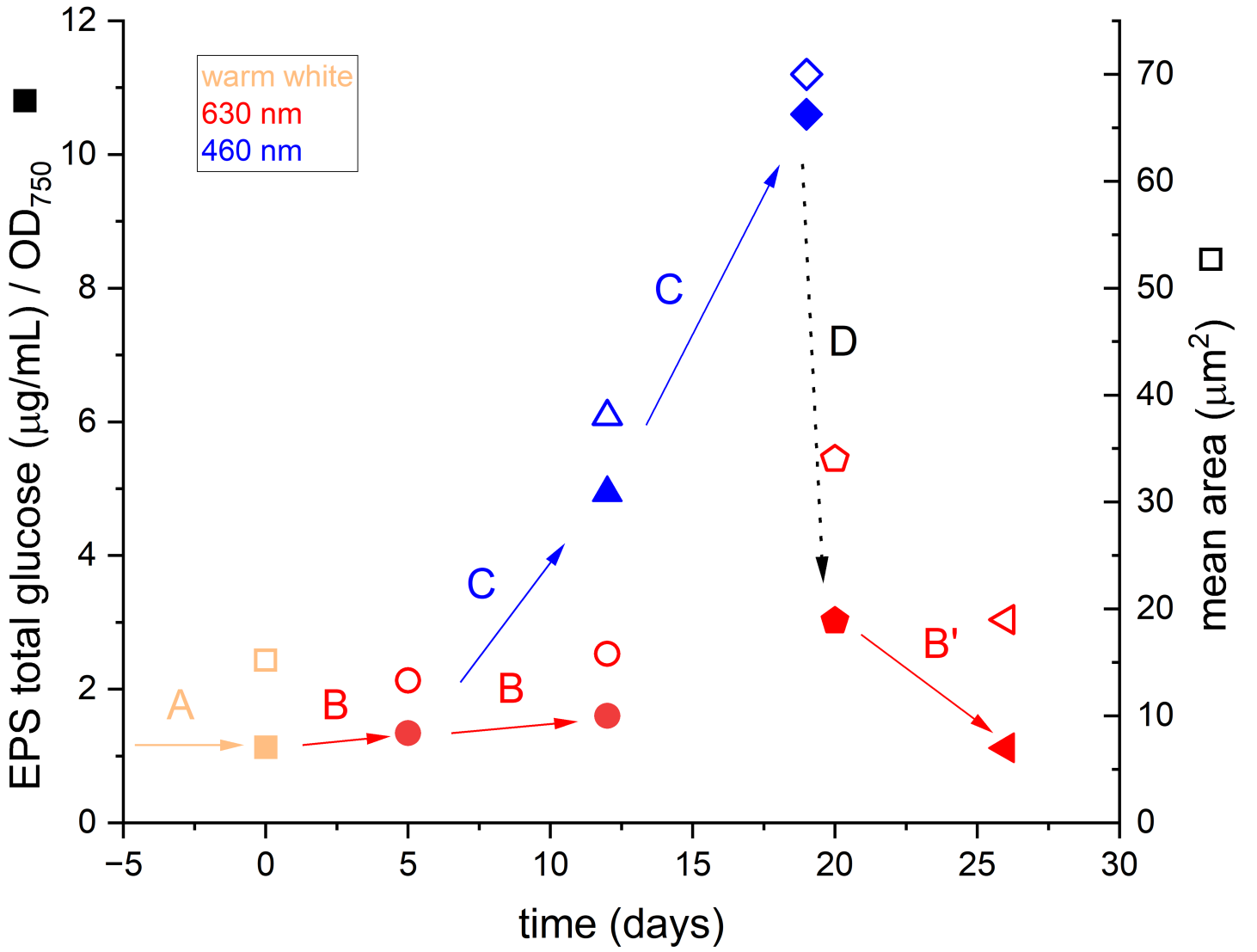


Figure 4

EPS levels (closed symbols) and mean aggregate areas (open symbols) in *Synechocystis*cultures grown under a changing light regime. A *Synechocystis* culture was pre-cultivated under warm-white light for 5 days (A), followed by subsequent cultivation under 630 nm red light for 5 days (B), 460 nm blue light for 11 days (C), a 5-fold dilution (D), and subsequent re-cultivation under 630 nm red light (B'). Light intensities at each step were set to 25 µmol photons m^{-2} s^{-1}. Arrows indicate the sequence of cultivation steps. Symbols denote individual sampling times at each cultivation phase.

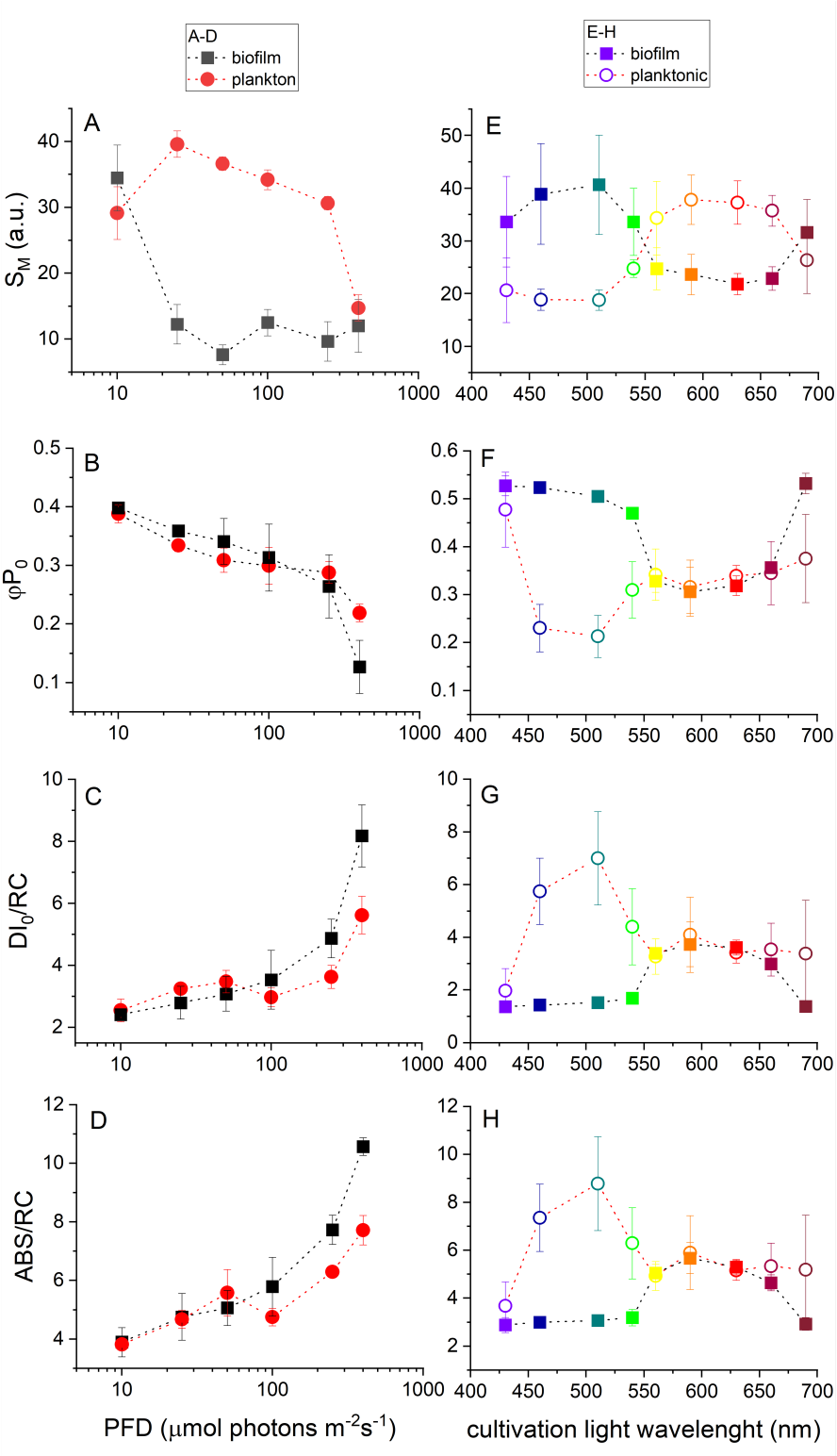


Figure 5

PSII photochemistry and energy fluxes in planktonic and biofilm *Synechocystis* cells under various growth light intensities (A–D) and wavelengths (E–H). Chlorophyll fluorescence parameters were derived from fast fluorescence induction (OJIP) curves recorded after dark acclimation. (A, E) Total complementary area (S_M = Area/(F_M-F_0)), representing the normalized area above the OJIP curves, which is proportional to the pool size of electron acceptors in the photosynthetic electron transport

chain. (B, F) Maximum quantum yield of PSII photochemistry ($\varphi P_0 = F_V/F_M = (F_M - F_O)/F_M$). (C, G) Flux of energy dissipated in processes other than trapping per PSII reaction center (DI_0/RC). (D, H) Apparent antenna size per active PSII reaction center ($ABS/RC = (M_0/V_J)/\varphi P_0$). The values represent mean ± SD (n = 3).

Supplementary Files

This is a list of supplementary files associated with this preprint. Click to download.

- SynechocystisBiofilmSupplement.docx